Pol. J. Environ. Stud. Vol. 34, No. 1 (2025), 985-997
DOI: *10.15244/pjoes/186645* ONLINE PUBLICATION DATE: 2024-09-02

Original Research

Experimental Study on Composition and Optic of Secondary Organic Aerosol Generated by Aqueous Photoxidation of Toluene in Presence of Copper Ions

Mincong Zhu[1], Mingqiang Huang[1*], Limei Zhang[1], Shunyou Cai[1], Weixiong Zhao[2], Changjin Hu[2], Xuejun Gu[2], Weijun Zhang[2]**

[1]Fujian Provincial Key Laboratory of Modern Analytical Science and Separation Technology, College of Chemistry & Chemical Engineering and Environment, Minnan Normal University, Zhangzhou 363000, China
[2]Laboratory of Atmospheric Physico-Chemistry, Anhui Institute of Optics and Fine Mechanics, Chinese Academy of Sciences, Hefei 230031, China

Received: 22 September 2023
Accepted: 29 March 2024

Abstract

Toluene and other aromatics can dissolve in atmospheric aqueous phases and undergo photooxidation reactions, forming secondary organic aerosol (SOA) after water evaporation. Copper ion is a typical heavy metal ion and is able to change the composition and optics of SOA. The reaction solution for OH-initiated photooxidation of toluene in presence of copper ions is atomized by TSI 9302, and the water is absorbed by silica gel to simulate the formation of aqueous SOA particles in this study. The composition and optics of the formed aqueous SOA are on-line and off-line, characterized by mass spectrometry and spectroscopy. Experimental results demonstrate that laser desorption/ionization mass spectra for aqueous SOA contain molecular ion peaks at m/z = 108, 124, and 140 for cresol, mehtyl dihydroxybenzene, and methyl trihydroxybenzene. The absorption peak intensity of phenolic compounds at 277 nm in the UV-Vis spectra of the collection solution for aqueous SOA increases, and electrospray ionization negative ion mass spectra show the polymer ion peak as high as m/z = 641. These indicate that copper ions catalyze the production of more phenolic compounds and hydroxyphenyl ether polymers formed by the polymerization of cresol. These products have the capacity for strong light absorption, leading to a significant increase in the averaged mass absorption coefficient (<MAC>) in 200-600 nm for aqueous SOA, which gently rises with an increment of copper ions. These provide the basis for studying the components and optics of aqueous SOA in presence of heavy metal ions.

Keywords: toluene, secondary organic aerosol, aqueous photoxidation, copper ion, optical properties.

*e-mail: huangmingqiang@mnnu.edu.cn
**e-mail: wjzhang@aiofm.ac.cn
Tel.: +86-596-2591445; Fax: +86-596-2591337

Introduction

Aromatic hydrocarbons such as benzene, toluene, and ethylbenzene emitted by solvent volatilization, vehicle exhaust, and other anthropogenic sources are usually organic pollutants in the atmosphere [1, 2]. They are inherently toxic and harmful to human health [3, 4]. Some aromatic compounds discharged into the atmosphere exist in the gas phase and are mainly oxidized by OH radicals to form semi-volatile and non-volatile organics. These organics then form secondary organic aerosol (SOA) by self-condensation or gas-particle partitioning [5, 6]. The other part of aromatic compounds dissolves in liquid aerosol, water droplets, clouds, and mist, then undergoes photooxidation to generate phenols, organic acids, and other low volatile products. These products remain in the particle phase after water evaporation, leading to the formation of SOA particles [7, 8]. SOA can scatter and absorb sunlight, reduce visibility, and have become a driving factor that interferes with regional climate [9, 10]. The contribution of SOA generated by aqueous reactions to atmospheric SOA is comparable to that of SOA formed from gaseous reactions and can explain the results of field observations that cannot be interpreted by gaseous formation methods [11, 12]. With the increasing impact of climate change, the study on the formation and optics of aqueous SOA has turned into a hot topic in atmospheric chemistry.

With the acceleration of urbanization, a large amount of heavy metal dust and fine particles have been emitted from human sources such as industry and transportation [13]. The heavy metal components in these fine particles are converted into soluble metal ions via atmospheric processes [14]. The field measurement results indicate that Cu, Fe, Ni, etc. are usual heavy metal ions in atmospheric aerosols [15]. Heavy metal ions have a catalytic effect, and OH, HO_2 radicals, and other reactive oxygen species (ROS) can be produced by Fenton-like chemical catalysis of H_2O_2 and O_3, affecting the oxidation potential of the atmosphere [16-18]. ROS participate in the oxidation of atmospheric VOCs and the aging process of aerosol particles, thereby impacting the components and optics of aqueous SOA.

Experiments conducted by Nguyen et al. [19] confirmed that when Fe^{2+} ions were present in the aqueous reaction system of glycolaldehyde and hydrogen peroxide, glycolic acid, oxalic acid, and other carboxylic acids significantly increased, and the oxygen - carbon ratio (O/C) for the formed aqueous SOA was as high as 0.90. Kameel et al. [20] found that Fe^{2+} ions can catalyze the aqueous reaction of isoprene with hydrogen peroxide to generate polyols, aldehydes, and carboxylic acids, thereby remarkably promoting the formation of aqueous SOA. Zhang et al. [21] demonstrated through field measurement experiments using an aerosol mass spectrometer that Fe^{3+} ions containing aerosol particles can promote the production of oxalate, glyoxylate, and other oxidized organic compounds. While Nimer et al. [22], Ling et al. [23], and Al-Abadleh et al. [24] found that Fe^{3+} ions could promote methoxyphenol and catechol to form secondary brown carbon products via complexation, polymerization, and other aqueous reactions. However, the above experiments [19-24] only focus on the influences of heavy metal ions on the chemical components of aqueous SOA. The optical properties of aqueous SOA in presence of heavy metal ions need to be further studied.

Toluene is the most abundant aromatic compound in the atmosphere. The chemical composition and reaction mechanism for OH-initiated photooxidation of toluene to form SOA particles in atmospheric photochemical reactions have been studied detailedly using a smog chamber [6, 25-28]. The Henry constant of toluene in the aqueous phase at room temperature is 1.4×10^{-3} mol• m^{-3}•Pa^{-1} [29], which has certain water solubility and can be dissolved in rainwater, liquid aerosol, and other aqueous phases [30]. Although Heath et al. [31] have carried out a study of the effects of temperature, pH, and other factors on the aqueous reaction rate of benzene and OH radicals and the yield of phenol, the effects of heavy metal ions on the aqueous reaction products of aromatic compounds still need to be further studied. Copper is a common heavy metal element, mainly derived from garbage incineration and biomass combustion. Copper mainly exists in the form of Cu^{2+} ions in aqueous phases [13, 15], nevertheless, the influences of Cu^{2+} ions on the formation and composition of aqueous SOA are fewly reported.

Our group used TSI 9302 to atomize the mixed solution of aldehydes and inorganic ammonium salts and dried it via a silica gel diffusion tube to generate SOA particles. Components of aqueous SOA are on-line and off-line, detected using mass spectrometry and spectroscopy; 4-methyl-imidazole and other imidazoles are identified [32]. On this basis, on-line and off-line apparatus is used to measure constituents of SOA generated by aqueous photoxidation of toluene in presence of Cu^{2+} ions in the current study. The averaged mass absorption coefficient (<MAC>) of aqueous SOA in 200-600 nm is measured by solvent extraction-continuous spectroscopy, as proposed by Updyke et al. [33] and Powelson et al. [34], and the influences of Cu^{2+} ions on the composition and optics of aqueous SOA are investigated. These provide the basis for studying the components and optics of aqueous SOA in presence of heavy metal ions.

Experimental Procedures

Materials

Toluene (> 99%), copper chloride (> 99%), hydrogen peroxide (30%), and hydrochloric acid (36%~38%) are all bought from China National Pharmaceutical Group Chemical Reagent Co., Ltd.

SOA Generated by Aqueous Photoxidation of Toluene in Presence of Copper Ions

Experiments are carried out in a homemade aqueous SOA generation device, shown in Fig. 1. The device consists of an aqueous reactor, an atomizer, a diffusion dryer, and a detection system [32]. The pH of 1 L of mixed solution for hydrogen peroxide, toluene, and copper chloride with a certain concentration is adjusted to 5 by hydrochloric acid (pH in atmospheric aqueous is about 5 [35]) and then transferred to an aqueous reactor under ultraviolet irradiation for a certain time. The aqueous reactor is a cylinder made of organic glass with a 25.5 cm height, a 9.0 cm diameter, and a 1.26 L volume. Its top is a detachable cover with a sampling port and a UV lamp placement port. The UV lamp adopts an integrated immersion UV lamp (Philips Lighting Electronics (Shanghai) Co., Ltd.) with a 2.8 cm diameter, 9.6 cm luminous area length, and 6 W power. The emitted ultraviolet wavelength range is 200-300 nm with a central wavelength of 254 nm. Under the irradiation of ultraviolet light, H_2O_2 photolysis generates OH radicals [36], which initiate the aqueous photooxidation reaction of toluene. The aqueous reactor is placed on a magnetic stirrer and magnetically stirred at 800 revolutions per minute to ensure that reaction products are evenly mixed. After illumination, the reaction solution is shifted to the TSI 9302 atomizer, atomized at a certain pressure to produce aerosol particles, and diffused through a silica gel drying tube to generate SOA particles.

Component and Optic Characterization of Aqueous SOA Particles

In all experiments, the concentrations of 20 μmol/L toluene and 100 μmol/L hydrogen peroxide are kept unchanged, and 0.25, 0.50, 1, 2, 3, 4, 5, and 6 μmol/L copper chloride are added to the mixed solution successively. After 180 minutes of UV irradiation for each mixture, as shown in Fig.1, the product solution is atomized with TSI 9302, and SOA particles are acquired through a silica gel drying tube. The generated SOA then enters an aerosol laser time-of-flight mass spectrometer (ALTOFMS) for measurement of size and composition. Also, aqueous SOA particles are collected in a wash bottle containing 10 mL of a 2% methanol solution for 3 hours to obtain the collection solution. The mass spectra of the collection solution are measured with a liquid chromatography mass spectrometer (LC-MS, Agilent-1200, Agilent-6320, USA). This instrument adopts electrospray ionization (ESI) with a measuring range of m/z = 5-1700 amu. The resolution is greater than 6900 and has a scanning speed of 4000 amu·s^{-1} [37]. Referring to our previous experiment [37], absorption spectra in 200 - 600 nm and organic carbon concentration (C_{mass}) for the collection solution are measured by a UV-visible spectrometer (UV-6100s, Shanghai Mapada Instruments Co., LTD.) and a total organic carbon analyzer (TOC-L, Shimadzu Company Co., LTD.). Mass absorption coefficient (MAC) parameters are obtained via the optical length, absorbance, and organic carbon concentration of the collection solution [33, 34].

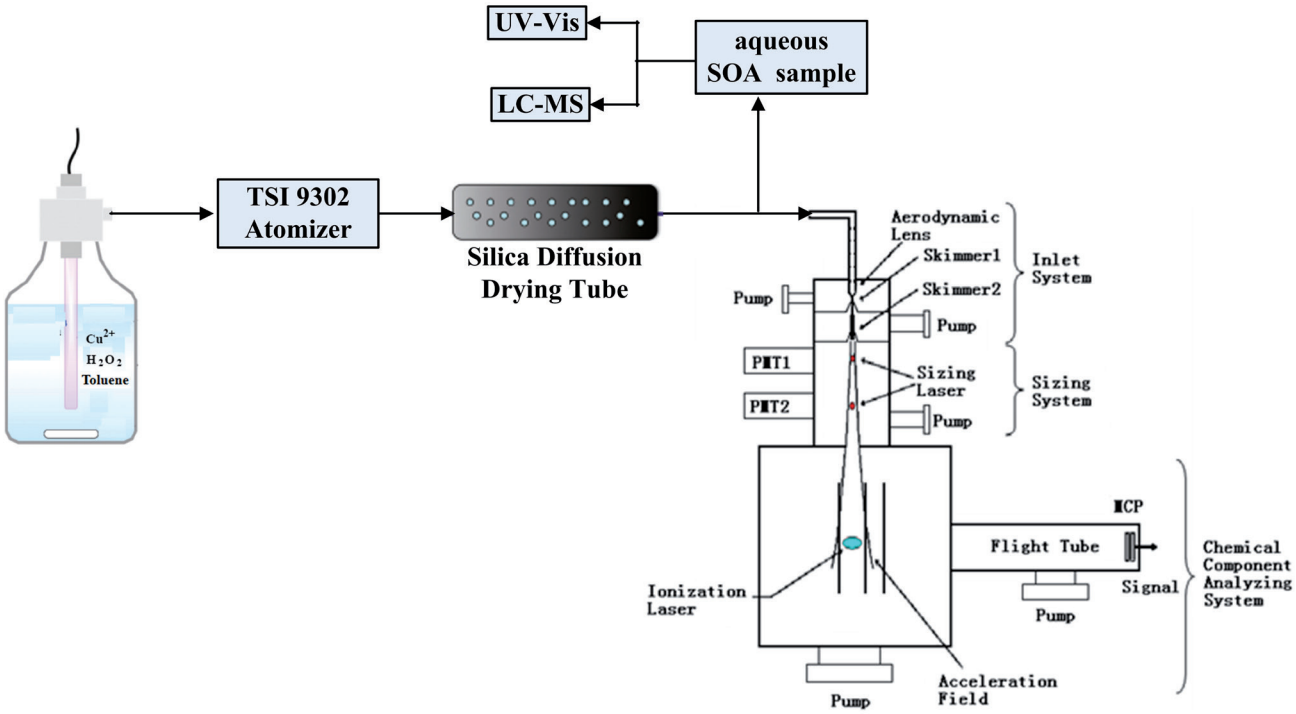

Fig. 1. Experimental schematic diagram of SOA particles formed from the aqueous photooxidation of toluene.

$$MAC(\lambda) = \frac{A^{solution}(\lambda) \times \ln 10}{b \times C_{mass}} \quad (1)$$

$$\langle MAC \rangle = \frac{1}{(\lambda_2 - \lambda_1)} \times \int_{\lambda_1}^{\lambda_2} MAC(\lambda) d\lambda \quad (2)$$

Where $A^{solution}(\lambda)$ in equation (1) is the absorbance of collection solution at λ, b for optical length (1 cm for this study). According to equation (2), MAC(λ) is integrated in the range of λ_1 - λ_2 and divided by ($\lambda_2 - \lambda_1$) to get the averaged MAC (<MAC>) in the λ_1 - λ_2 range.

Results and Discussion

For confirming aqueous photooxidation products of toluene, UV irradiation of (1) 20 μmol/L toluene, (2) 100 μmol/L hydrogen peroxide, (3) 20 μmol/L toluene with 100 μmol/L hydrogen peroxide, and (4) a dark reaction of 20 μmol/L toluene with 100 μmol/L hydrogen peroxide are carried out. UV - Vis absorption spectra of aqueous product solutions after 3 hours of reaction are shown in Fig. 2. There is no absorption peak in the UV - Vis spectrum of hydrogen peroxide after 3 hours of illumination. UV irradiation of toluene and the dark reaction of toluene and hydrogen peroxide in a mixed solution both only have strong a absorption band near 204 nm. This band is characteristic of the absorption formed from the superposition of the π → π* transition and the vibrational energy level transition of the benzene ring [38]. This indicates that toluene does not react with H_2O_2 in the aqueous phase. In addition to the characteristic absorption band of the benzene ring near 204 nm, a new absorption band appears near 277 nm in the UV-Vis spectrum of the aqueous reaction solution between toluene and hydrogen peroxide under UV irradiation. As suggested by Marković et al. [39], this band is the characteristic absorption formed from the n → π* transition the between oxygen atom in a phenolic compound and the C=C bond on the benzene ring. This demonstrates that an aqueous solution contains phenolic compounds. UV irradiation of hydrogen peroxide produces OH radicals [36], which initiate the aqueous photooxidation of toluene to form phenolic products. Then, the aqueous solution is shifted to the atomizer to generate SOA particles.

On-line Characterization of Components for Aqueous SOA Particles

According to the design principle of ALTOFMS, as illustrated in Fig.1, aqueous SOA particles enter the sizing system through an aerodynamic lens and two skimmers, and successively encounter two 532 nm lasers at a certain distance. The generated scattered light is received by a photomultiplier tube, and the travel velocity of SOA particles is calculated by a timing circuit to obtain their size. Subsequently, SOA particles get into the vacuum chamber and are desorbed/ionized by a 248 nm laser. The resulting ions are measured by a time-of-flight mass spectrometer, and component information about SOA particles is acquired from ion peaks in the mass spectrum. Due to the power density of the 248 nm laser, which is in the order of 10^8 W/cm^3, it has strong energy and desorption ionizes the components of SOA particles, leading to the fragmentation of molecular ions, so the mass peak of fragment ions is mainly obtained [27, 40].

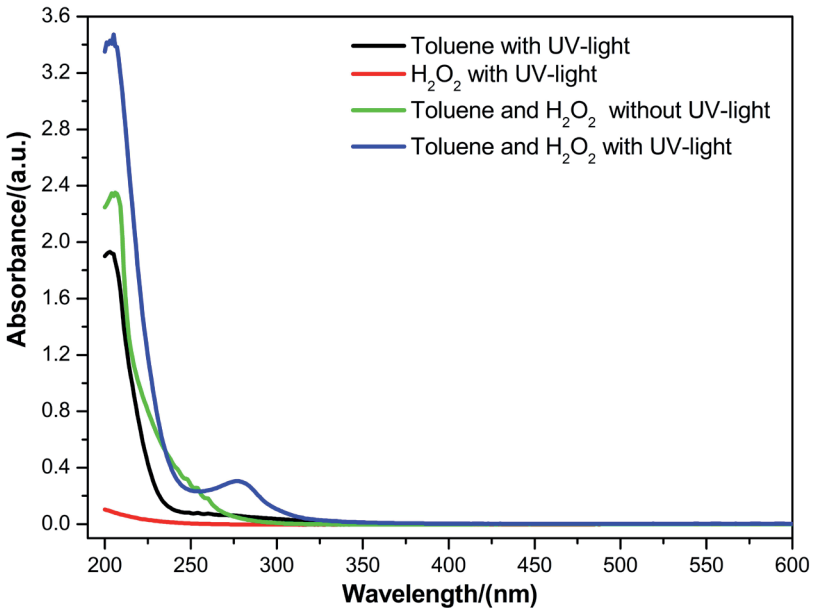

Fig. 2. UV-Vis absorption spectra of toluene and hydrogen peroxide aqueous photooxidation experiment and control experiments solutions.

Averaged positive ion mass spectra for 200 SOA particles generated by aqueous photoxidation of 20 μmol/L toluene and 100 μmol/L hydrogen peroxide measured on-line by ALTOFMS are shown in Fig. 3. Apart from organic carbon fragment peaks (m/z = 12 (C^+) and 24 (C_2^+)), the mass spectra of aqueous SOA particles have fragment ion peaks at m/z = 29, 43, and 57 in the range of m/z less than 60. According to the experimental results of our previous studies [27, 41], these mass peaks correspond to fragment ion peaks of HCO^+ (m/z = 29), CH_3CO^+ (m/z = 43), and $HCOCO^+$ (m/z = 57) produced by the ionization of carbonyl compounds such as glyoxal and methylglyoxal. This suggests that aqueous SOA particles contain carbonyl compounds. Also, the mass spectra of aqueous SOA particles contain characteristic ion peaks for the phenolic compounds at m/z = 93 ($C_6H_5O^+$), benzene ion and its fragment peaks at m/z = 77 ($C_6H_5^+$), m/z = 65 ($C_5H_5^+$), and m/z = 39 ($C_3H_3^+$) [27, 41]. Also, these ion peaks have larger peak areas than those of m/z=29, 43, and 57, indicating that phenolic compounds have a higher content and are the main components in aqueous SOA particles.

When 4 μmol/L Cu^{2+} ions are present in the mixed solution of 20 μmol/L toluene with 100 μmol/L hydrogen peroxide, the averaged positive ion mass spectra for 200 aqueous SOA particles are illustrated in Fig. 4. The peak of m/z = 64 has the highest intensity, corresponding to the peak of the Cu^+ ion, while m/z = 80, with relatively strong intensity is the CuO^+ ion peak [42]. Except for fragment peaks of organic carbon (m/z = 12,24) and carbonyl compounds (m/z = 29,43), characteristic peaks for phenolic compounds (m/z = 93), and the benzene ion and its fragment peaks (m/z = m/z = 77,39), mass peaks at m/z = 108, 124, and 140 are newly emerging when compared to Fig. 3. Peaks of m/z = 108 may be considered molecular ion peaks of cresol ($CH_3C_6H_4OH^+$), while m/z = 124 and 140 are 16 and 32 more than m/z = 108, which may refer to molecular ion peaks of mehtyl dihydroxybenzene ($CH_3C_6H_3(OH)_2^+$) and methyl trihydroxybenzene ($CH_3C_6H_2(OH)_3^+$). It can be inferred that phenolic compounds such as cresol, mehtyl dihydroxy benzene and methyl trihydroxybenzene are the main components of SOA particles generated by aqueous photoxidation of toluene in presence of Cu^{2+} ions. In order to characterize compositions of aqueous SOA in detail, off-line measurements are performed.

Off-line Characterization of Components for Aqueous SOA Particles

UV-Vis spectra of collection solutions for SOA generated by aqueous photoxidation of toluene in presence of different concentrations of Cu^{2+} ions are displayed in Fig. 5. In absence of Cu^{2+} ions, the UV-Vis spectrum of the collection solution for aqueous SOA is similar to that of the toluene photooxidation solution shown in Fig. 2, with absorption peaks near 204 and 277 nm, which confirms that phenolic compounds are the main components in aqueous SOA particles. OH radicals produced by photolysis of hydrogen peroxide under ultraviolet irradiation initiate the addition reaction of toluene in the aqueous phase, as illustrated in Fig. 6. OH radicals are added to the benzene ring to form the OH-toluene adduct, and the hydrogen atom of the adduct is extracted by oxygen molecules to generate cresol. According to the experimental results of the aqueous photooxidation reaction of phenol and other phenolic compounds conducted by Sun et al. [43], the OH radical can continue to react with cresol to produce cresol oxygen radicals. This radical nucleophilic attacks cresol to form 2,3'-dimethyl-4'-hydroxy-diphenyl ether.

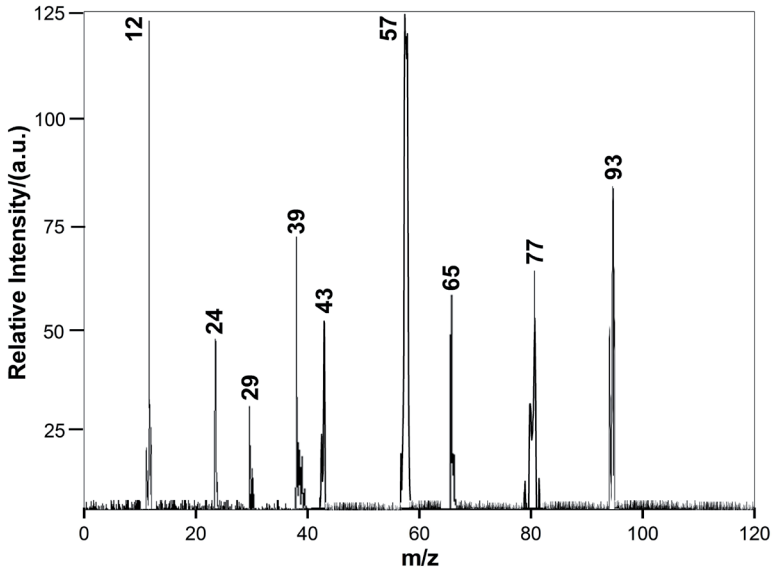

Fig. 3. Averaged positive ion mass spectra for 200 SOA particles generated by aqueous photooxidation of toluene in absence of copper ions.

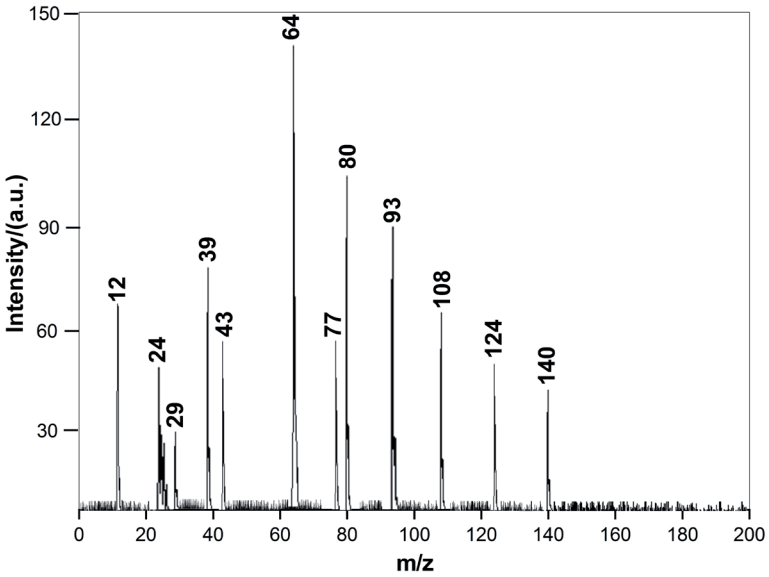

Fig. 4. Averaged positive ion mass spectra for 200 SOA particles generated by aqueous photooxidation of toluene in presence of 4 μmol/L copper ions.

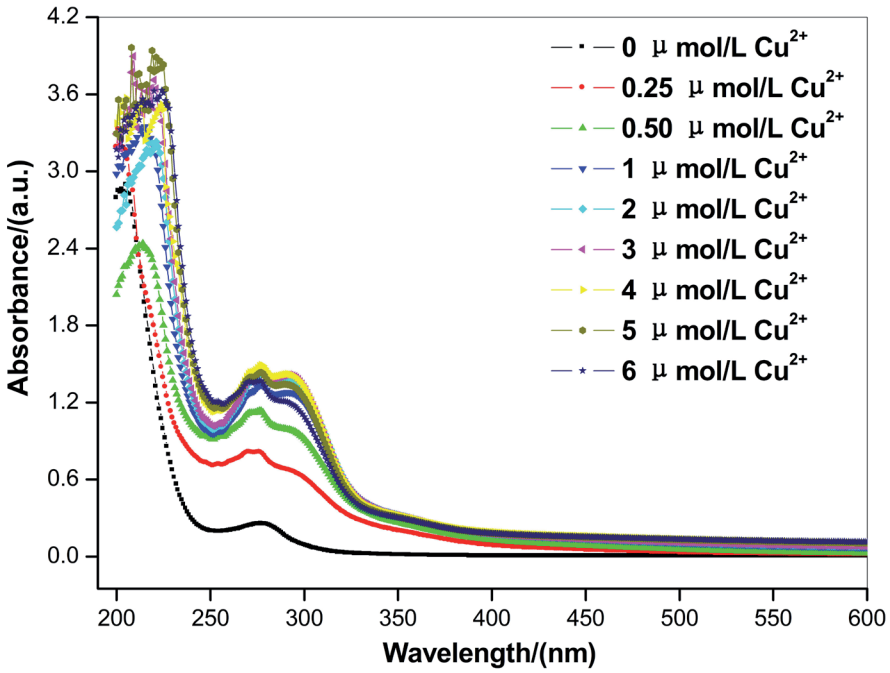

Fig. 5. UV-Vis absorption spectra of collection solutions for SOA particles generated by aqueous photooxidation of toluene in presence of different concentration of copper ions.

In addition, oxygen molecules can also be added to the OH-toluene adduct to form peroxy radicals, which undergo isomerization to generate oxygen bridge radicals and produce 2-butendial and methylglyoxal through ring fracture reactions. Therefore, cresol, aromatic ether, and aldehyde compounds are the products of aqueous photooxidation of toluene initiated by OH radicals. These products have low volatility and remain in the particle phase to form SOA after water evaporation [7, 8].

The collection solution of aqueous SOA particles is not separated by a chromatographic column and directly enters a mass spectrometer to measure the mass spectra after electrospray ionization. Electrospray ionization is a soft ionization technology that will not break the molecular ion peak by using a low-voltage method. The negative ionization mode causes the measured organic molecule to dissociate and lose hydrogen ions, resulting in a deprotonated molecular ion peak ([M-H]$^-$), providing information on the molecular weight of

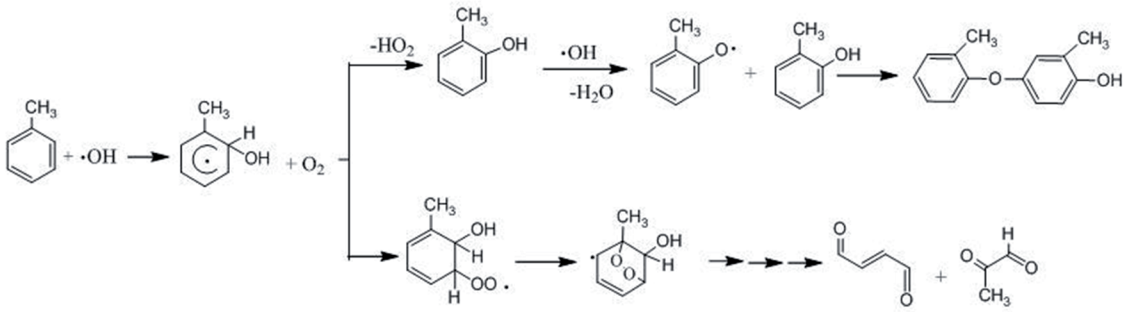

Fig. 6. Possible reaction mechanism for formation of phenolic and aldehyde compounds by aqueous photooxidation of toluene initiated by OH radical.

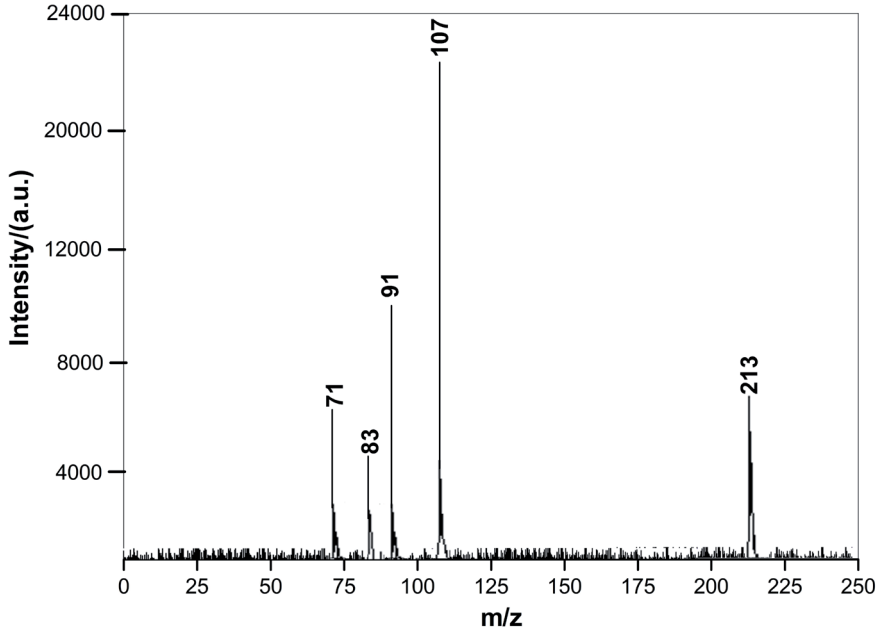

Fig. 7. Electrospray ionization negative ion mass spectra of SOA particles generated by aqueous photooxidation of toluene in absence of copper ions.

the measured component [35]. Electrospray negative ion mass spectra for the collection solution of aqueous SOA in absence of Cu^{2+} ions shown in Fig. 7 emerge $[M-H]^-$ peaks at m/z = 71, 83, 91, 107, and 213. Among them, the peak of m/z = 91 may refer to the unreacted deprotonated molecular ion peak of toluene ($C_6H_5CH_2^-$). In view of the possible reaction mechanism between toluene and OH radicals displayed in Fig. 6 and the molecular weight information of the products, the strongest mass peak at m/z = 107 is considered the deprotonated molecular ion peak of cresol ($CH_3C_6H_4O^-$). While peaks at m/z = 71, m/z = 83, and m/z = 213 may refer to deprotonated molecular ion peaks of methylglyoxal (CH_3COCO^-), 2-butendial ($HCOCH{=}CHCO^-$), and 2,3'-dimethyl-4'-hydroxy-diphenyl ether ($C_{14}H_{13}O_2^-$). These further verify the existence of cresol, aromatic ether, and aldehyde compounds in SOA particles generated by the aqueous photoxidation of toluene in absence of Cu^{2+} ions.

When there are Cu^{2+} ions of different concentrations in an aqueous system, as shown in Fig. 5, the absorption curve of each collection solution of aqueous SOA particles does not change significantly, but the absorbance of each collection solution at 277 nm is greater than that of a solution without Cu^{2+} ions. As can be seen from Fig. 5, when the concentration of Cu^{2+} is in the range of 0.25 - 4 μmol/L, the absorbance of collection solution at 277 nm gradually increases with an increment of Cu^{2+} ions. In absence of Cu^{2+} ions, the absorbance of collection solution for aqueous SOA particles at 277 nm is 0.254, while in presence of 4 μmol/L Cu^{2+} ions, the absorbance of the collection solution at 277 nm is 1.489, about 6 times that of the absence of Cu^{2+} ions. These show that the content of phenolic compounds in aqueous SOA particles increases significantly when Cu^{2+} is present in the aqueous system. This is mainly because Cu^{2+} ions belong to fourth-period transition-state metal ions and have catalytic effects.

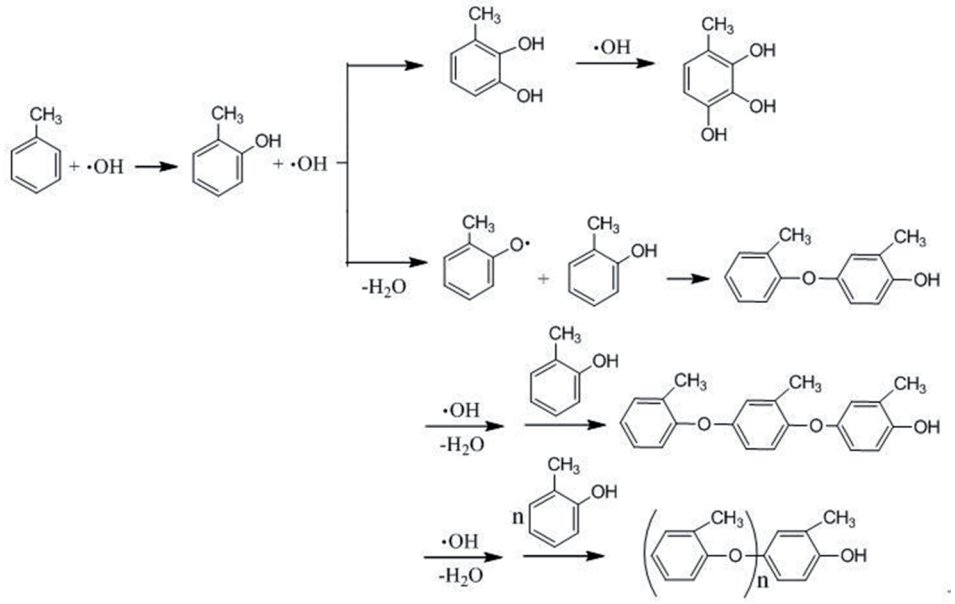

Fig. 8. Possible reaction mechanism for formation of polyhydroxyphenols and hydroxyphenyl ether polymers by aqueous photooxidation of toluene initiated by OH radical.

They form Fenton-like reagents with hydrogen peroxide, and the Cu element catalyzes hydrogen peroxide to produce OH radicals through the conversion of Cu^{2+} and Cu^{+} valence states [44]. Therefore, when Cu^{2+} ions are present in an aqueous system, hydrogen peroxide can generate more OH radicals under ultraviolet irradiation and Cu^{2+} ion catalysis. As illustrated in Fig. 8, the OH radical undergoes an addition reaction with toluene, and the OH radical is added to the benzene ring to form cresol. The excessive OH radicals then continue to react with cresol to produce polyhydroxyphenol products such as dihydroxybenzene and trihydroxybenzene [45]. The resulting aqueous SOA contains more phenolic compounds and the absorbance of the collection solution at 277 nm increases significantly. Due to the constant concentration of hydrogen peroxide and toluene in each experiment, when the concentration of Cu^{2+} ions increases to a certain concentration (4 μmol/L), hydrogen peroxide is fully catalyzed to produce OH radicals, and the absorbance of the collection solution at 277 nm reaches its maximum value. Afterward, when the concentration of Cu^{2+} ions continues to increase, the amount of OH radicals formed almost stays constant, so the absorbance of the collection solution at 277 nm basically remains unchanged.

In order to characterize the chemical components of SOA particles generated by aqueous photoxidation of toluene in presence of 4 μmol/L Cu^{2+} ions in detail, off-line electrospray ionization mass spectrometry is carried out, and the negative ion mass spectra measured are shown in Fig. 9. Apart from peaks of m/z = 71 (methylglyoxal deprotonation molecular ion (CH_3COCO^-) peak), m/z = 83 (2-butendial deprotonation molecular ion ($HCOCH{=}CHCO^-$) peak), m/z = 107 (cresol deprotonation molecular ion ($CH_3C_6H_4O^-$) peak), and m/z = 213 (2,3'- dimethyl-4'-hydroxy diphenyl ether deprotonation molecular ion ($C_{14}H_{13}O_2^-$) peak), there are strong peaks of m/z = 123, 139, 320, 427, 534, and 641. According to the reaction mechanism shown in Fig. 9 and the molecular weight information of the products, m/z = 123 and 139 are considered deprotonated molecular ion peaks for mehtyl dihydroxybenzene ($CH_3C_6H_4O_2^-$) and methyl trihydroxybenzene ($CH_3C_6H_4O_3^-$). Also, the mass charge ratio of m/z = 213, 320, 427, 534, and 641 differs by 107, which may refer to deprotonated molecular ion peaks of hydroxy-phenyl ether polymers. On the basis of the experimental results of Sun et al. [43], as displayed in Fig. 8, OH radicals can react with cresol to generate cresol oxygen radicals, which nucleophilically attacks cresol to produce hydroxyphenyl ether dimer (2,3'-dimethyl-4'- hydroxy-diphenyl ether), which generates deprotonated molecular ions ($C_{14}H_{13}O_2^-$, m/z = 213) by electrospray ionization. Similarly, under the activation of OH radicals, hydroxyphenyl ether dimers continue to react with cresol to produce hydroxyphenyl ether trimers (producing deprotonated molecular ion $C_{21}H_{20}O_3^-$, m/z = 320), tetramers (producing deprotonated molecular ion $C_{28}H_{27}O_4^-$, m/z = 427), pentamers (producing deprotonated molecular ion $C_{35}H_{34}O_5^-$, m/z = 534), and hexamers (producing deprotonated molecular ion $C_{42}H_{41}O_6^-$, m/z = 641). These further confirm that Cu^{2+} ions catalyze the production of more OH radicals from hydrogen peroxide, leading to an increase in the generation of mehtyl dihydroxybenzene and methyl trihydroxybenzene and triggering the polymerization of cresol to form high molecular weight products of hydroxyphenyl ether polymers.

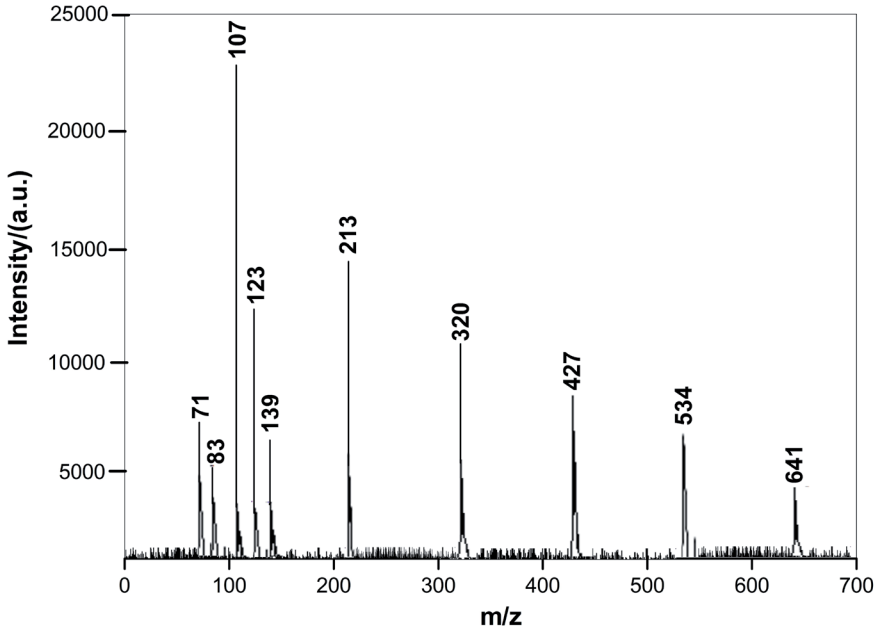

Fig. 9. Electrospray ionization negative ion mass spectra of SOA particles generated by aqueous photooxidation of toluene in presence of 4 μmol/L copper ions.

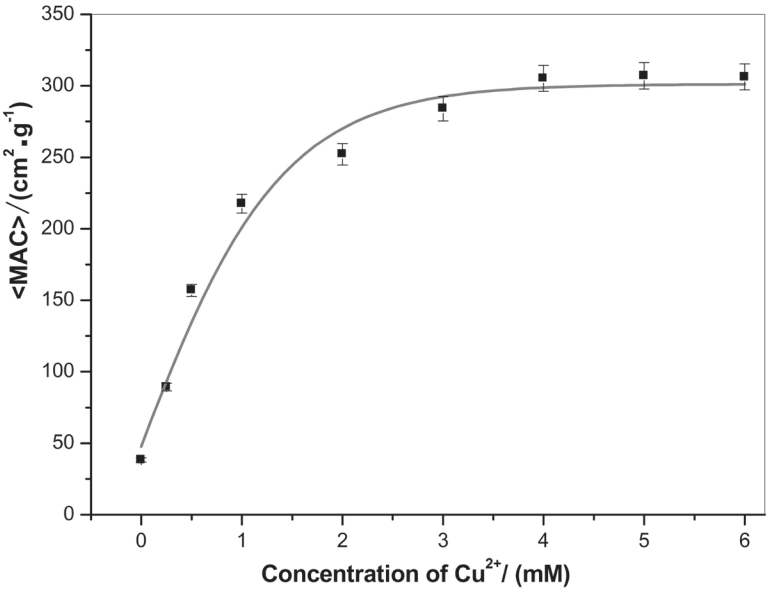

Fig. 10. Averaged mass absorption coefficient (<MAC>) of SOA particles generated by aqueous photooxidation of toluene in presence of different concentration of copper ions.

Optical Characterization of Aqueous SOA Particles

Aerosol particles affect climate change via light absorption, and the averaged mass absorption coefficient (<MAC>) is often used to characterize the impact of particles on light absorption [33, 34]. The total organic carbon concentration of the collection solution for SOA generated by aqueous photoxidation of toluene in presence of different concentrations of Cu^{2+} ions is measured using a TOC-L analyzer. Combined with the UV-Vis absorption spectra for the collection solution at 200-600 nm shown in Fig. 5, <MAC> is obtained according to equations (1) and (2). As shown in Fig. 10, when Cu^{2+} ions are not present, the <MAC> of SOA generated by aqueous photoxidation of toluene in 200-600 nm is 38 cm^2/g, which is a bit higher than that of 1,3,5-trimethylbenzene SOA formed in absence of NO*x,* measured by Updyke et al. [33] (20 cm^2/g). The <MAC> of aqueous SOA particles obviously increases when Cu^{2+} ions are present in the system and gradually

increases with an increment of Cu^{2+} ions. However, when the concentration of Cu^{2+} ions exceeds 4 μmol/L, the optical properties of aqueous SOA particles tend to be stable.

Phenolic compounds have a C=C bond and electron-removing functional group of -OH in the benzene ring, which can absorb photons and have a certain degree of light absorption ability. The greater the number of -OH functional groups contained in a phenolic compound molecule, the stronger its light absorption ability [46]. According to the above chemical component detection results, the major constituents of SOA generated by aqueous photoxidation of toluene in absence of Cu^{2+} ions are cresol, aromatic ether, and aldehyde compounds. These product molecules only have C=C and C=O bonds, without strong chromophores or color aids. They contain a small number of -OH functional groups. Thus, aqueous SOA particles have weak absorption abilities [46]. When Cu^{2+} ions are present in an aqueous system, Cu^{2+} ions catalyze the production of OH radicals from hydrogen peroxide. As the concentration of Cu^{2+} ions increases, the catalytic ability increases, and the number of OH radicals formed in the system increases, resulting in an increase in the formation of mehtyl dihydroxybenzene, methyl trihydroxybenzene, and hydroxyphenyl ether polymers formed by the polymerization of cresol. These products contain a large number of -OH functional groups, thus enhancing their ability to absorb light, resulting in an increment of <MAC> for the generated aqueous SOA particles. Due to the constant concentration of toluene and hydrogen peroxide in each experiment, when Cu^{2+} ions rise to a certain concentration (4 μmol/L), they catalyze the majority of hydrogen peroxide to produce OH radicals, and the <MAC> of formed aqueous SOA particles reaches a maximum value of 306 cm^2/g, which is a little higher than that of ammonia-aged aromatic SOA reported by Updyke et al. [33] (~300 cm^2/g). Since then, the concentration of Cu^{2+} ions has continued to rise, but OH radicals no longer increase. The formed polyhydroxyphenols and hydroxyphenyl ether polymers remained basically unchanged, and the optics of aqueous SOA particles tended to stabilize.

It is noteworthy that some researchers have recently carried out studies on the formation and aging of toluene and other aromatic SOA [47-50]. Mitra et al. [47] have investigated the effects of water vapors, active nitrogen, and acidity on the light-absorbing components and optics of toluene SOA and found that the mass absorption cross-section (MAC) of toluene SOA increased with [NO*x*/ΔHC]. Also, under the condition of 80% RH, acidity facilitated the production of brown carbon components, while the presence of ammonia led to an increase in MAC for toluene SOA. Wang et al. [48] have studied the influences of ferric chloride fine particles on the components and optics of toluene SOA. They observed that methylcatecol and other phenolic compounds produced by the photooxidation of toluene will condense on surfaces for ferric chloride fine particles and then combine with iron ions to form metallo-organic complexes with strong light absorption ability. As a result, the yield of toluene SOA increased, and the light absorption ability of SOA (MAC) was enhanced significantly. Campbell et al. [49] have coated the surface of $CuSO_4$ and $FeSO_4$ seed particles with β-pinene and naphthalene SOA particles and used two novel online instruments to quantify the OH radical and reactive oxygen species produced. The effects of metal-organic interaction and particle-phase chemistry on the oxidative potential (OP) of SOA were studied. They found a range of antagonistic and synergistic interactions for Fe(II), Cu(II) and SOA, highlighting metal-ascorbate and naphthoquinone-ascorbate reactions as vital drivers of OP. Malecha and Nizkorodov [50] have collected 135-trimethylbenzene, isoprene, and other anthropogenic and biogenic SOA particles in uncoated CaF_2 windows as substrates, annealed and aged by direct photolysis by UV-LED. Oxygenated volatile organic compounds such as acetaldehyde, acetone, formic acid, and acetic acid were detected during the photodegradation of SOA particles. They estimate that under summer conditions in Los Angeles, SOA would lose at least 1% of its mass during photolysis within a 24-hour period. The photodegradation process of SOA would affect the budget of gaseous organic compounds in the atmosphere.

However, the above experiments focus on the study of SOA produced by gaseous photooxidation of toluene and other volatile organic compounds. Compared with these studies [47-50], based on the solubility of toluene in liquid aerosol, rainwater, and other aqueous phases, the device shown in Fig. 1 is used to carry out the aqueous photooxidation reaction of toluene in presence of Cu^{2+} ions in this study. The reaction product solution was atomized by TSI 9302, and atmospheric aqueous SOA particles were simulated to form after water evaporation. The composition and optics of the formed aqueous SOA are on-line and off-line, characterized by mass spectrometry and spectroscopy. ALTOFMS on-line measurement combined with UV-Vis absorption spectroscopy and electrospray ionization mass spectrometry are used for off-line detection to verify that the main components of SOA particles generated by aqueous photoxidation of toluene in presence of Cu^{2+} ions are polyhydroxyphenols and hydroxyphenyl ether polymers. These experimental results are consistent with those of Chang et al. [45]. Their results showed that the infrared spectra for aqueous reaction products of phenol and other phenolic compounds initiated by hydroxyl radicals are similar to those of aerosol light-absorbing substances of humic-like substances (HULIS) measured in the field. The hydroxyphenyl ether polymer formed from the aqueous reaction of phenolic compounds is one of the major sources of HULIS in aerosol particles. Especially in industrial areas heavily polluted by automobile exhaust, there are high concentrations of aromatic compounds and heavy metal fine particles in the atmosphere. Under conditions of

high humidity, toluene, and other aromatic compounds may undergo similar aqueous reactions to form polyhydroxyphenols and hydroxyphenyl ether polymers. These products have strong absorbance, thereby altering the components and optics of aerosol particles and thus affecting atmospheric visibility, causing the generation of haze pollution.

Conclusions

The TSI 9302 atomizer is used to atomize the reaction solution for OH-initiated aqueous photooxidation of toluene in presence of Cu^{2+} ions in this study, and SOA particles are generated after removing water through a diffusion drying tube. Components and optics of aqueous SOA particles are characterized by ALTOFMS, UV-Vis, and LC-MS, and the effects of Cu^{2+} ions on components and <MAC> in 200-600 nm of aqueous SOA are also investigated. The results show that the main components of SOA particles generated by aqueous photoxidation of toluene in presence of Cu^{2+}ions are cresol, mehtyl dihydroxybenzene, methyl trihydroxybenzene, and hydroxyphenyl ether polymers formed by polymerization of cresol. The content of these products and the <MAC> of aqueous SOA gradually increase with an increment of Cu^{2+} ions. When the concentration of Cu^{2+} ions in the aqueous system is 4 μmol/L, the <MAC> of the formed aqueous SOA particles is 306 cm^2/g, which is close to <MAC> of ammonia-aged aromatic SOA reported in the literature. However, the <MAC> of aqueous SOA particles is detected by the off-line method, and the subsequent experiments can carry out on-line detection of the absorption coefficient and other optical parameters for aqueous SOA particles.

Acknowledgments

Our work was supported by the National Natural Science Foundation of China (No. 42275136), the Natural Science Foundation of Fujian Province of China (No. 2021J01987, 2020J02044). The authors also express our gratitude to the referees for their valuable comments.

Conflict of Interest

The authors declare no conflict of interest.

Reference

1. GHOSH B., DE M., ROUT T.K., PADHY P.K. Study on spatiotemporal distribution and health risk assessment of BTEX in urban ambient air of Kolkata and Howrah, West Bengal, India: Evaluation of carcinogenic, non-carcinogenic and additional leukaemia cases. Atmospheric Pollution Research. **14** (10), 101878, **2023**.
2. BIAN Y., ZHANG Y., ZHOU Y., FENG X.S. BTEX in the environment: An update on sources, fate, distribution, pretreatment, analysis, and removal techniques. Chemical Engineering Journal. **435** (1), 134825, **2022**.
3. QIU H., CHUANG K.J., FAN Y.C., CHANG T.P., CHUANG H.C., WONG E.L.Y., BAI C.H., HO K.F. Association between ambient BTEX mixture and neurological hospitalizations: A multicity time-series study in Taiwan. Ecotoxicology and Environmental Safety. **263**, 115239, **2023**.
4. PARTHA D.B., CASSIDY-BUSHROW A.E., HUANG Y.X. Global preterm births attributable to BTEX (benzene, toluene, ethylbenzene, and xylene) exposure. Science of The Total Environment. **838** (4), 156390, **2022**.
5. BEHNAMI A., JAFARI N., BENIS K.Z., FANAEI F., ABDOLAHNEJAD A. Spatio-temporal variations, ozone and secondary organic aerosol formation potential, and health risk assessment of BTEX compounds in east of Azerbaijan Province, Iran. Urban Climate. **47**,101360, **2023**.
6. LI Y.X., ZHAO J.Y., WANG Y., SEINFELD J.H., ZHANG R.Y. Multigeneration production of secondary organic aerosol from toluene photooxidation. Environmental Science & Technology. **55** (13), 8592, **2021**.
7. LI F.H., ZHOU S.Z., DU L., ZHAO J., HANG J., WANG X.M. Aqueous-phase chemistry of atmospheric phenolic compounds: A critical review of laboratory studies. Science of The Total Environment. **856** (1), 158895, **2023**.
8. MOUCHEL-VALLON C., BRÄUER P., CAMREDON M., VALORSO R., MADRONICH S., HERRMANN H., AUMOUNT B. Explicit modeling of volatile organic compounds partitioning in the atmospheric aqueous phase. Atmospheric Chemistry and Physics. **13** (2), 1023, **2013**.
9. ANDREAE M.O., RAMANATHAN V. Climate's dark forcings. Science. **340** (6130), 280, **2013**.
10. MOISE T., FLORES J.M., RUDICH Y. Optical properties of secondary organic aerosols and their changes by chemical processes. Chemical Reviews. **115** (10), 4400, **2015**.
11. XU W.Q., HAN T.T., DU W., WANG Q.Q., CHEN C., ZHAO J., ZHANG Y.J., LI J., FU P.Q., WANG Z.F., WORSNOP D.R., SUN Y. Effects of aqueous-phase and photochemical processing on secondary organic aerosol formation and evolution in Beijing, China. Environmental Science & Technology. **51** (2), 762, **2017**.
12. ERVENS B., TURPIN B.J., WEBER R.J. Secondary organic aerosol formation in cloud droplets and aqueous particles (aqSOA): a review of laboratory, field and model studies. Atmospheric Chemistry and Physics. **11** (21), 11069, **2011**.
13. GUAN Q.Y., LI F.C., YANG L.Q., ZHAO R., YANG Y.Y., LUO H.P. Spatial-temporal variations and mineral dust fractions in particulate matter mass concentrations in an urban area of northwestern China. Journal of Environmental Management. **222**, 95, **2018**.
14. TANG M.J., CZICZO D.J., GRASSIAN V.H. Interactions of water with mineral dust aerosol: Water adsorption, hygroscopicity, cloud condensation, and ice nucleation. Chemical Reviews. **116** (7), 4205, **2016**.
15. FOMBA K.W., VAN PINXREREN D., MÜLLER K., LINUMA Y., LEE T., COLLETT JR J.L., HERRMANN H. Trace metal characterization of aerosol particles and cloud water during HCCT 2010. Atmospheric Chemistry and Physics. **15** (7), 8751, **2015**.
16. HARRIS E., SINHA B., VAN PINXTEREN D., TILGNER A., FOMBA K.W., SCHNEIDER J., ROTH A., GNAUK

T., FAHLBUSCH B., MERTES S., LEE T., COLLETT J., FOLEY S., BORRMANN S., BORRMANN S., HOPPE P., HERRMANN H. Enhanced role of transition metal ion catalysis during in-cloud oxidation of SO_2. Science. **340** (6133), 727, **2013**.
17. ENAMI S., SAKAMOTO Y., COLUSSI A.J. Fenton chemistry at aqueous interfaces. Proceedings of the National Academy of Sciences of the United States of America. **112** (2), 623, **2014**.
18. TANG M.J., HUANG X., LU K.D., GE M.F., LI Y.H., CHENG P., ZHU T., DING A.J., ZHANG Y.H., GLIGOROVSKI S., SONG W., DING X., BI X., WANG X.M. Heterogeneous reactions of mineral dust aerosol: implications for tropospheric oxidation capacity. Atmospheric Chemistry and Physics. **17** (19), 11727, **2017**.
19. NGUYEN T.B., COGGON M.M., FLAGAN R.C., SEINFELD J.H. Reactive uptake and photo-Fenton oxidation of glycolaldehyde in aerosol liquid water. Environmental Science & Technology. **47** (9), 4307, **2013**.
20. KAMEEL F.R., RIBONI F., HOFFMANN M.R., ENAMI S., COLUSSI A.J. Fenton oxidation of gaseous isoprene on aqueous surfaces. Journal of Physical Chemistry C. **118** (50), 29151, **2014**.
21. ZHANG G.H., LIN Q.H., PENG L., YANG Y.X., JIANG F., LIU F.X., SING W., CHEN D.H., CAI Z., BI X.H., MILLER M., TANG M.J., HUANG W.L., WANG W.X., PENG P.A., SHENG G.Y. Oxalate formation enhanced by Fe-containing particles and environmental implications. Environmental Science & Technology. **53** (3), 1269, **2019**.
22. NIMER A.A., ROCHA L., RAHMAN M.A., NIZKORODOV S.A., AL-ABADLEH H.A. Effect of oxalate and sulfate on iron-catalyzed secondary brown carbon formation. Environmental Science & Technology. **53** (12), 6708, **2019**.
23. LING J.Y., SHENG F., WANG Y., PENG A.P., JIN X., GU C. Formation of brown carbon on Fe-bearing clay from volatile phenol under simulated atmospheric conditions. Atmospheric Environment. **228**, 117427, **2020**.
24. AL-ABADLEH H.A. Aging of atmospheric aerosols and the role of iron in catalyzing brown carbon formation. Environmental Science: Atmospheres. **1** (6), 297, **2021**.
25. LIN P., LIU J.M, SHILLING J.E., KATHMANN S.M., LASKIN J., LASKIN A. Molecular characterization of brown carbon (BrC) chromophores in secondary organic aerosol generated from photo-oxidation of toluene. Physical Chemistry Chemical Physics. **17** (36), 23312, **2015**.
26. JI Y.M., ZHAO J., TERAZONO H., MISAWA K., LEVITT N.P., LI Y.X., LIN Y., PENG J.F., WANG Y., DUAN L., PAN, B., ZHANG F., FENG X.D., AN T.C., MARRERO -ORTIZ W., SECREST J., ZHANG A.L., SHIBUYA K., MOLINA M.J., ZHANG R.Y. Reassessing the atmospheric oxidation mechanism of toluene. Proceedings of the National Academy of Sciences of the United States of America. **114** (31), 8169, **2017**.
27. XU J., HUANG M.Q., FENG Z.Z., CAI S.Y., ZHAO W.X., HU C,J., GU X,J., ZHANG W.J. Effects of inorganic seed aerosol on the formation of nitrogen-containing organic compounds from reaction of ammonia with photooxidation products of toluene. Polish Journal of Environmental Studies. **29** (1), 907, **2020**.
28. SRIVASTAVA D., LI W.R., TONG S.R., SHI Z.B., HARRISON R.M. Characterization of products formed from the oxidation of toluene and m-xylene with varying NO*x* and OH exposure. Chemosphere. **334**,139002, **2023**.
29. LI J.Q., SHEN C.Y., WANG H.M., HAN H.Y., ZHENG P.C., XU G.H., JIANG H.H., CHU Y.N. Dynamic measurements of Henry′s law constant of aromatic compounds using proton transfer reaction mass spectrometry. Acta Physico-Chimica Sinica. **24** (4), 705, **2008**.
30. ŠOŠTARĆ A., STOJIĆ A., STOJIĆ S.S., GRŽETIĆ I. Quantification and mechanisms of BTEX distribution between aqueous and gaseous phase in a dynamic system. Chemosphere. **144**, 721, **2016**.
31. HEATH A.A., EHRENHAUSER F.S., VALSARAJ K.T. Effects of temperature, oxygen level, ionic strength, and pH on the reaction of benzene with hydroxyl radicals in aqueous atmospheric systems. Journal of Environmental Chemical Engineering. **1** (4), 822, **2013**.
32. ZHU M.C., HUANG M.Q., LU T.T., CAI S.Y., SHAN X.B., SHENG L.S., ZHAO W.X., GU X,J., ZHANG W.J. Experimental study on the imidazoles of aqueous secondary organic aerosol formed from reaction of methylglyoxal and ammonium sulphate. Atmospheric Pollution Research. **13** (9), 101535, **2022**.
33. UPDYKE K.M., NGUYEN T.B, NIZKORODOV S.A. Formation of brown carbon via reactions of ammonia with secondary organic aerosols from biogenic and anthropogenic precursors. Atmospheric Environment. **63,** 22, **2012**.
34. POWELSON M.H., ESPELIEN B.M, HAWKINS L.N., GALLOWAY M.M., DE HAAN D.O. Brown carbon formation by aqueous-phase carbonyl compound reactions with amines and ammonium sulfate. Environmental Science & Technology. **48** (2), 985, **2014**.
35. CARLTON A.G., TURPIN B.J., ALTIERI K.E., SEITZINGER S., REFF A., LIM H.J., ERVENS B. Atmospheric oxalic acid and SOA production from glyoxal: Results of aqueous photooxidation experiments. Atmospheric Environment. **41** (35), 7588, **2007**.
36. AO X.L., LIU W.J. Degradation of sulfamethoxazole by medium pressure UV and oxidants: Peroxymonosulfate, persulfate, and hydrogen peroxide. Chemical Engineering Journal. **313** (1), 629, **2017**.
37. ZHANG W., HUANG M.Q., LU T.T., CAI S.Y., ZHAO W.X., HU C.J., GU X.J., ZHANG W.J. Characterization of nitro-aromatic compounds of ethylbenzene secondary organic aerosol with acidic sodium nitrate fine particles. Polish Journal of Environmental Studies. **31** (1), 451, **2022**.
38. KINAYTÜRK N.Y., KALAYCI T., TUNALI B., ALTUĞ D.T. A spectroscopic approach to compare the quantum chemical calculations and experimental characteristics of some organic molecules; Benzene, toluene, p-xylene, p-toluidine. Chemical Physics. **570**, 111905, **2023**.
39. MARKOVIĆ S., TOŠOVIĆ J. Application of time-dependent density functional and natural bond orbital theories to the UV–vis absorption spectra of some phenolic compounds. Journal of Physical Chemistry A. **119** (35), 9352, **2015**.
40. XU J., HUANG M.Q., CAI S.Y., LIU X.Q., HU C,J., GU X,J., FANG L., ZHANG W.J. Mass spectral analysis of the aged 1,3,5-trimethylbenzene secondary organic aerosol in the presence of ammonium sulfate seeds. Polish Journal of Environmental Studies. **26** (4), 1531, **2017**.
41. HUANG M.Q., HAO L.Q., CAI S.Y., GU X.J., ZHANG W.X., HU C.J., WANG Z.Y., FANG L., ZHANG W.J. Effects of inorganic seed aerosols on the particulate products of aged 1,3,5-trimethylbenzene secondary organic aerosol. Atmospheric Environment. **152**, 490, **2017**.
42. ARNDT J., DEBOUDT K., ANDERSON A., BLONDEL A., ELIET S., FLAMENT P., FOURMENTIN M., HEALY

R.M., SAVARY V., SETYAN A., WENGER J.C. Scanning electron microscopy-energy dispersive X-ray spectrometry (SEM-EDX) and aerosol time-of-flight mass spectrometry (ATOFMS) single particle analysis of metallurgy plant emissions. Environmental Pollution. **210**, 9, **2016**.

43. SUN Y.L., ZHANG Q., ANASTASIO C., SUN J. Insights into secondary organic aerosol formed via aqueous-phase reactions of phenolic compounds based on high resolution mass spectrometry. Atmospheric Chemistry and Physics. **10** (2), 4809, **2010**.
44. SINGH D.K., GUPTA T. Role of ammonium ion and transition metals in the formation of secondary organic aerosol and metallo-organic complex within fog processed ambient deliquescent submicron particles collected in central part of Indo-Gangetic Plain. Chemosphere. **181**, 725, **2017**.
45. CHANG J.L., THOMPSON J.E. Characterization of colored products formed during irradiation of aqueous solutions containing H_2O_2 and phenolic compounds. Atmospheric Environment. **44** (4), 541, **2010**.
46. LASKIN A., LASKIN J., NIZKORODOV S.A. Chemistry of atmospheric brown carbon. Chemical Reviews. **115** (10), 4335, **2015**.
47. MITRA K., MISHRA H.R., PEI X.Y., PATHAK R.K. Secondary organic aerosol (SOA) from photo-oxidation of toluene: 1 influence of reactive nitrogen, acidity and water vapours on optical properties. Atmosphere. **13** (7), 1099, **2022**.
48. WANG W.C., HUANG M.Q., HU H.M., ZHAO W.X., HU C.J., GU X.J., ZHANG W.J. Characterization of chemical components and optical properties of toluene secondary organic aerosol in presence of ferric chloride fine particles. Atmosphere. **14** (7), 1075, **2023**.
49. CAMPBELL S.J., UTINGER B., BARTH A., PAULSON S.E., KALBERER M. Iron and copper alter the oxidative potential of secondary organic aerosol: insights from online measurements and model development. Environmental Science & Technology. **57** (36), 13546, **2023**.
50. MALECHA K.T., NIZKORODOV S.A. Photodegradation of secondary organic aerosol particles as a source of small, oxygenated volatile organic compounds. Environmental Science & Technology. **50** (18), 9990, **2016**.